

A thymus candidate in lampreys

Baubak Bajoghli¹, Peng Guo^{2,3}, Narges Aghaallaei¹, Masayuki Hirano^{2,3}, Christine Strohmeier¹, Nathanael McCurley^{2,3}, Dale E. Bockman⁴, Michael Schorpp¹, Max D. Cooper^{2,3} & Thomas Boehm¹

Immunologists and evolutionary biologists have been debating the nature of the immune system of jawless vertebrates—lampreys and hagfish—since the nineteenth century. In the past 50 years, these fish were shown to have antibody-like responses and the capacity to reject allografts¹ but were found to lack the immunoglobulin-based adaptive immune system of jawed vertebrates². Recent work has shown that lampreys have lymphocytes that instead express somatically diversified antigen receptors that contain leucine-rich-repeats, termed variable lymphocyte receptors (VLRs)^{3,4}, and that the type of VLR expressed is specific to the lymphocyte lineage: T-like lymphocytes express type A VLR (*VLRA*) genes, and B-like lymphocytes express *VLRB* genes⁵. These clonally diverse anticipatory antigen receptors are assembled from incomplete genomic fragments by gene conversion^{6–9}, which is thought to be initiated by either of two genes encoding cytosine deaminase⁹, cytosine deaminase 1 (*CDA1*) in T-like cells and *CDA2* in B-like cells⁵. It is unknown whether jawless fish, like jawed vertebrates, have dedicated primary lymphoid organs, such as the thymus, where the development and selection of lymphocytes takes place^{10,11}. Here we identify discrete thymus-like lympho-epithelial structures, termed thymoids, in the tips of the gill filaments and the neighbouring secondary lamellae (both within the gill basket) of lamprey larvae. Only in the thymoids was expression of the orthologue of the gene encoding forkhead box N1 (*FOXN1*)¹⁰, a marker of the thymopoietic microenvironment in jawed vertebrates¹², accompanied by expression of *CDA1* and *VLRA*. This expression pattern was unaffected by immunization of lampreys or by stimulation with a T-cell mitogen. Non-functional *VLRA* gene assemblies were found frequently in the thymoids but not elsewhere, further implicating the thymoid as the site of development of T-like cells in lampreys. These findings suggest that the similarities underlying the dual nature of the adaptive immune systems in the two sister groups of vertebrates extend to primary lymphoid organs.

The long-standing question of whether lampreys have a thymus led to the description of several circumscribed lymphoid accumulations in the gill basket of lamprey larvae as candidates for the thymus, for instance in the lateral branchial wall sinuses¹³ and the ‘thymic placode’ inside the epipharyngeal folds¹⁴ (Supplementary Information and Supplementary Fig. 1). However, histological surveys failed to reveal a thymus analogue unambiguously. We were prompted to re-examine the issue of a thymus equivalent in lampreys by the recent identification of two separate lineages of lymphocytes in lampreys, a finding indicating that the dual nature of the immune system extends to all vertebrates⁵. T-like cells of lampreys were shown to express *VLRA* on their surface (denoted *VLRA*⁺ cells), whereas B-like cells express surface and secreted forms of *VLRB*. Moreover, *VLRA*⁺ cells were shown to express *CDA1* preferentially, whereas *VLRB*⁺ cells express *CDA2* (ref. 5). With respect to a putative thymus primordium in jawless fish, the lamprey orthologue of *FOXN1*, a marker of the thymopoietic microenvironment in jawed vertebrates^{11,12}, was found to be expressed in lamprey larvae in a region of the gill basket where *VLRB*-expressing

lymphocytes could not be found¹⁰. On the basis of the cell-type specificity of gene expression in lamprey lymphocytes, we therefore hypothesized that co-expression of *VLRA* and *CDA1* or of *VLRB* and *CDA2* would distinguish the primary lymphoid organs in which these T-like and B-like cells are generated in jawless vertebrates.

Expression of the *VLR* genes was detectable by RNA *in situ* hybridization in cells of many tissues of European brook lamprey (*Lampetra planeri*) larvae. Cells expressing *VLRA* and *VLRB* messenger RNAs were found in the gill filaments, kidneys, typhlosole and blood (Fig. 1a, b). *VLRA*-expressing cells dominated in the gill basket, whereas *VLRB*-expressing cells were more frequent in the kidneys and typhlosole (Supplementary Fig. 2). These data are in agreement with previous flow cytometric analyses of cells from the closely related sea lamprey (*Petromyzon marinus*)⁵ and indicate a tissue-specific pattern of distribution for the two lymphocyte lineages.

Expression of the *CDA* genes was more spatially restricted than that of the *VLR* genes. When assayed by *in situ* hybridization, *CDA1* mRNA was detected at discrete sites that were located primarily at the tip of gill filaments. *CDA1* was not expressed by cells in the liver (not shown), kidneys, typhlosole, blood or other tissues outside the gill basket (Fig. 1c). Conversely, cells expressing *CDA2* were preferentially expressed in the typhlosole, predominantly around the central blood vessel, and occasionally expressed in the kidneys and blood (Fig. 1d), indicating that the sites of *CDA1* and *CDA2* expression do not overlap. The patterns of co-expression of *VLR* and *CDA* genes in these distinct anatomical sites (Fig. 1e) suggest that *VLRA*⁺ T-like cells might develop in the gill region, whereas *VLRB*⁺ B-like cells might originate in haematopoietic tissue, namely in the typhlosole and kidneys. This is reminiscent of the situation in jawed vertebrates, in which T cells develop in the thymus and B cells develop primarily in the bone marrow or its functional equivalents.

The thymus in jawed vertebrates is uniquely identifiable by thymocyte expression of recombination-activating genes (*RAGs*) during rearrangement of the genes that encode the T-cell antigen receptor, as well as by epithelial cell expression of the gene encoding the transcription factor *FOXN1*. It has previously been shown that the lamprey orthologue of the thymic epithelial marker *FOXN1*, designated *FOXN1* (or *FOXN4L*), is expressed in the epithelium of the gill basket of lamprey larvae¹⁰. To explore the possibility that a thymus-like structure might be found in the gill basket of lamprey larvae, we searched for sites at which markers of thymic epithelial cells (*FOXN1* and Delta-like B (*DLL-B*)) and of lymphocytes (*VLRA* and *CDA1*) were expressed together. All four genes were found to be expressed in the same region of the gill filaments (Fig. 2a). Double *in situ* hybridization confirmed the association of *VLRA* and *CDA1* expression in the thymoids and indicated that some *VLRA*-expressing cells also express *CDA1*. By contrast, *VLRB*-expressing cells do not express *CDA1* (Fig. 2b) and are absent from the thymoid region (Figs 1b and 2b). To examine the micro-anatomical relationship between epithelial and lymphocyte markers, we used a *DLL-B* probe that specifically detects the expression of a putative *FOXN1* target gene encoding a Delta-related Notch

¹Department of Developmental Immunology, Max Planck Institute of Immunobiology and Epigenetics, Stuebeweg 51, D-79108 Freiburg, Germany. ²Emory Vaccine Center, 954 Gatewood Road, Atlanta, Georgia 30329, USA. ³Department of Pathology and Laboratory Medicine, Emory University, 1462 Clifton Road North-East, Atlanta, Georgia 30322, USA. ⁴Department of Cellular Biology and Anatomy, Medical College of Georgia, Augusta, Georgia 30912, USA.

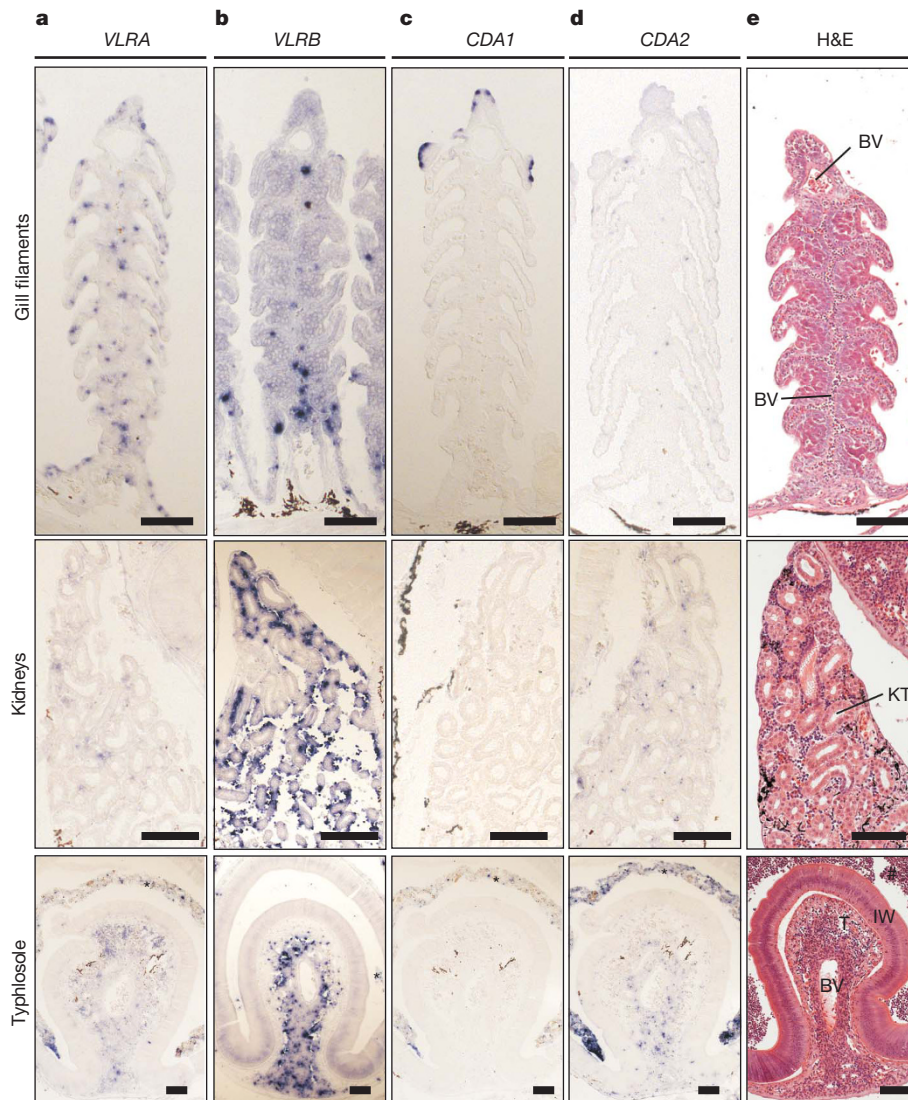


Figure 1 | Tissue-specific expression of VLR and CDA genes in *L. planeri* larvae. **a–d**, Gene-specific expression, as determined by RNA *in situ* hybridization with gene-specific riboprobes, is shown in blue. **a**, VLRA expression. **b**, VLRB expression. **c**, CDA1 expression. **d**, CDA2 expression. **e**, Histological structure. Haematoxylin and eosin (H&E) staining of sections

equivalent to those used for RNA *in situ* hybridization. The intestinal contents (*) (primarily yeast) cause non-specific staining in **a–d** and are also seen in **e** (#). BV, blood vessel; IW, intestinal wall; KT, kidney tubule; T, typhlosole. Scale bars, 100 μ m.

ligand¹⁰, as a marker of epithelial cells, and CDA1, as a marker of developing T-like cells. In the thymoid, these cells are located in close proximity (Fig. 2c). Analysis by immunofluorescence confirmed the presence of VLRA-producing cells and the absence of VLRB-producing cells in the thymoid, whereas both cell types were found in blood vessels (Fig. 2d). Histological analysis by light microscopy showed that the thymoid contains both epithelial cells and lymphocytes (Fig. 2e). Electron micrographs confirmed that these cells are present in close proximity in the thymoid (Fig. 2f) and indicate that phagocytosis of cellular debris occurs at this site (Fig. 2g). Only a small subset of CDA1-expressing cells proliferate (Supplementary Fig. 3), suggesting cell-cycle-specific regulation of this lamprey gene belonging to the AID–APOBEC family. Cells expressing CDA1 were found in the tips of the gill filaments encompassing the entire gill basket (Fig. 2h and Supplementary Fig. 4), indicating that the thymoids are not confined to a specific pharyngeal arch. These findings in *L. planeri* were confirmed for *P. marinus* (Supplementary Fig. 5), indicating that the specific gene expression patterns are a general characteristic of

lampreys. We conclude that the lympho-epithelial structure identified in the gill basket bears the diagnostic hallmarks expected for a thymus equivalent: namely expression of CDA1 (a gene that is predicted to be associated with somatic diversification of the VLRA locus) together with VLRA expression, and the concordant expression of FOXP1 with DLL-B (one of the key target genes of FOXP1).

In jawed vertebrates, the thymus is a primary lymphoid organ, which, unlike secondary lymphoid tissues such as lymph nodes and the spleen, does not change its structure during an immune response. We applied this criterion to the thymoid. Lamprey larvae mount strong immune responses against various antigens, including the exo-sporium of *Bacillus anthracis*^{5,15}. Immunization with this antigen (Fig. 3a) leads to a general proliferative response in haematopoietic tissues¹⁵. There is a massive increase in cell proliferation in the typhlosole and kidneys, whereas the increase in the number of proliferating cells in the gill vasculature is more modest (Fig. 3b). Concomitantly, the number of VLRA-expressing cells increases in the typhlosole, and the number of VLRB-expressing cells increases in the blood vessels,

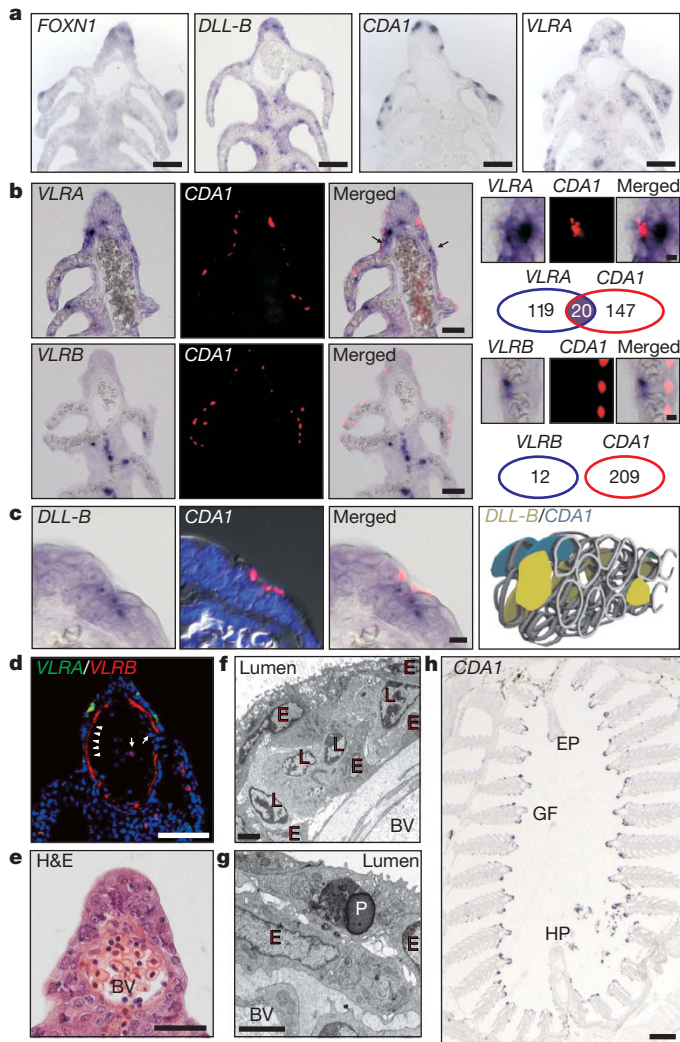


Figure 2 | Characterization of the lamprey thymoid. **a**, Concomitant expression of epithelial markers (*FOXN1* and *DLL-B*) and two lymphocyte-specific genes (*CDA1* and *VLRA*) at the tip of gill filaments, as determined by RNA *in situ* hybridization with gene-specific riboprobes. Scale bars, 50 μ m. **b**, Co-expression of *VLRA* (blue) and *CDA1* (red) in a subset of *VLRA*-expressing lymphocytes (upper panels), as determined by RNA *in situ* hybridization with gene-specific riboprobes on adjacent sections, which are shown separately and as a merged image. Co-expression seems to occur preferentially in cells expressing low levels of *VLRA* (arrows indicate co-expressing cells). *VLRB* (blue) and *CDA1* are not co-expressed (lower panels). Scale bars, 40 μ m. Greater magnifications are shown to the right (scale bars, 5 μ m) with quantitative assessments of gene expression presented underneath (numbers indicate number of cells that express one or both genes). **c**, Close proximity of cells expressing *DLL-B* (blue) and *CDA1* (red) in the thymoid. RNA *in situ* hybridization was carried out with gene-specific locked-nucleic-acid-enhanced oligonucleotides on adjacent sections, which are shown separately and as a merged image. For the *CDA1* panel, the images of the DNA counterstain (4',6-diamidino-2-phenylindole (DAPI), blue) and the differential interference contrast are superimposed. Scale bar, 10 μ m. The rightmost panel shows a three-dimensional reconstruction of thymoid tissue with *DLL-B*- and *CDA1*-expressing cells indicated in different colours; other cells are shown only in outline. **d**, Immunofluorescence microscopy with anti-*VLRA* (green) and anti-*VLRB* (red) antibodies. Intravascular lymphocytes are indicated by arrows. Deposits of *VLRB* at the vessel walls are indicated by arrowheads. DNA is counterstained with DAPI (blue). Scale bar, 50 μ m. **e**, Lympho-epithelial structure of the thymoid as revealed by light microscopy. Nucleated erythrocytes are visible in the large blood vessel (BV) underneath the thymoid. Scale bar, 30 μ m. **f**, Lympho-epithelial structure of the thymoid as revealed by transmission electron microscopy: lymphocytes (L), epithelial cells (E) and blood vessel (BV). The lumen of the gill chamber is at the top left. Scale bar, 2 μ m. **g**, Evidence for phagocytosis (P) in the thymoid. Scale bar, 2 μ m. **h**, *CDA1* expression is found at the tips of gill filaments (GF) and in the epithelial linings of the epipharyngeal ridge (EP) and the hypopharyngeal fold (HP), as shown by RNA *in situ* hybridization with a gene-specific riboprobe on a transverse section (see also Supplementary Fig. 4). Scale bar, 300 μ m. Sections are from *L. planeri* in **a** (*FOXN1*, *CDA1* and *VLRA*), **e** and **h**, and from *P. marinus* in all other panels.

being particularly noticeable in the cavernous bodies located at the base of gill filaments (Supplementary Fig. 6). After intracoelomic injection of phytohaemagglutinin (PHA) (Fig. 3a), this mitogen is distributed throughout the vasculature and rapidly accumulates in the gill region (Supplementary Fig. 7). PHA is known to cause a proliferative burst of *VLRA*⁺ cells⁵, and this general proliferative effect is clearly seen by using *in situ* analysis in the gill region, kidneys and typhlosole (Fig. 3b). Stimulation with PHA also increased the number of *VLRA*-expressing cells in the gill region, kidneys and typhlosole (Supplementary Fig. 6). Importantly, however, PHA does not induce proliferation of cells in the thymoid tips (Fig. 3b), and it does not change the pattern of *CDA1* expression (Fig. 3c). The finding that cells in the thymoids fail to respond to antigenic or mitogenic stimuli is compatible with the thymoid being a primary lymphoid organ rather than a secondary one.

We sought more direct evidence that the thymoid is the site at which T-like cells develop. We examined the status of *VLRA* gene assembly in this region and elsewhere. Previously, it has been shown that *VLRA*⁺ lymphocytes typically assemble only one *VLRA* allele⁵, the other allele being retained in the germ-line configuration. Furthermore, the assembled *VLRA* allele is almost always functional. Non-functional rearrangements of *VLRA* genes are exceedingly rare and are always accompanied by a functional assembly on the second allele¹⁶. This observation suggests a process that ensures the selective development of *VLRA*⁺ lymphocytes. We used laser-capture microdissection to procure genomic DNA from cells at the thymoid tip of the gill filament and, as a control, from within the blood vessels at the filament base (Fig. 4a). As anticipated, assembled *VLRA* genes could be amplified from the DNA isolated from both the thymoid and the blood.

Strikingly, however, non-functional sequences were found only in the thymoid fraction, whereas the sequences obtained from cells isolated from blood vessels were all functional (Fig. 4b and Supplementary Fig. 8). This difference indicates that non-functional assemblies impair the further development of *VLRA*⁺ lymphocytes. Indeed, within the gill basket, caspase-3-positive apoptotic cells were also found primarily in the gill filament tip and neighbouring secondary lamellae, closely resembling the distribution of *CDA1*-expressing cells (Fig. 4c). These findings are compatible with the idea of selection against thymoid cells that are undergoing non-functional *VLRA* assembly. It will be interesting to examine whether this is also true for *VLRB*, which was described recently and is structurally similar to *VLRA*¹⁷.

To evaluate the stringency of this selection process, we investigated whether non-functionally assembled *VLRA* genes could be identified in *VLRA*⁻*VLRB*⁻ cells isolated from the blood and gills. Although it was possible to amplify assembled *VLRA* genes from *VLRA*⁻*VLRB*⁻ cells with lymphocyte light-scattering features, two rounds of amplification were required to detect them (Fig. 4d). Essentially all of these relatively rare *VLRA* assemblies were non-functional, in contrast to the status of *VLRA* genes in *VLRA*⁺*VLRB*⁻ cells (Fig. 4e and Supplementary Fig. 9). Notably, *VLRA* assemblies were not found in *VLRA*⁻*VLRB*⁺ cells (Fig. 4d). Together, these findings indicate a remarkable efficiency of selection for *VLRA*⁺ cells.

Here we describe a previously unrecognized lympho-epithelial structure in the gill basket of lamprey larvae. The thymoid bears the hallmarks of a tissue where lymphocytes undergo *VLRA* assembly and selection for the expression of functional *VLRA* genes, which encode the anticipatory antigen receptor of T-like lymphocytes. Our findings suggest that this structure is a candidate for a thymus in lampreys. The dispersed nature and relatively inconspicuous morphological appearance of the lamprey thymoid structure could explain why it has gone unnoticed for so long

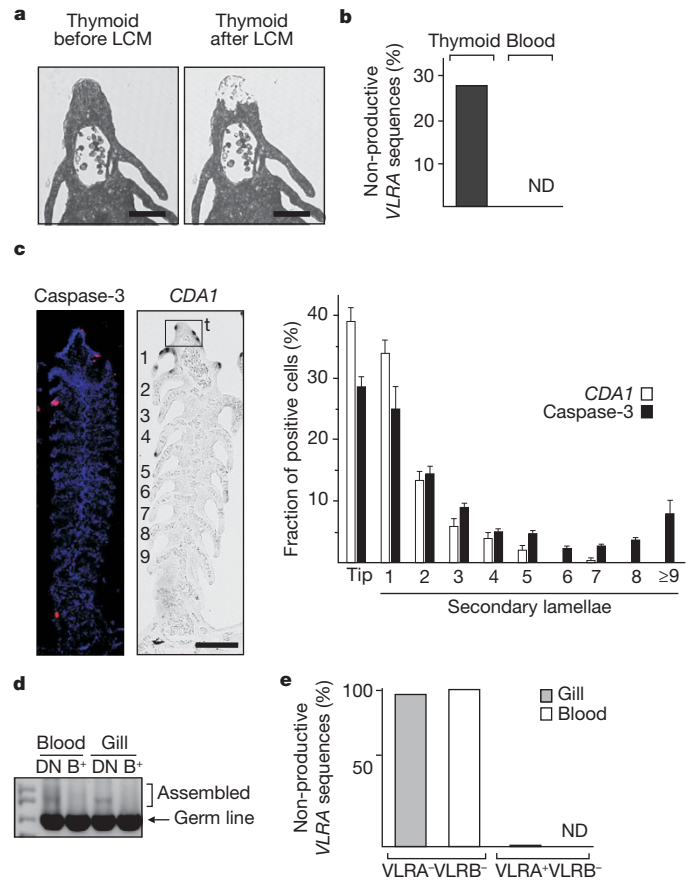
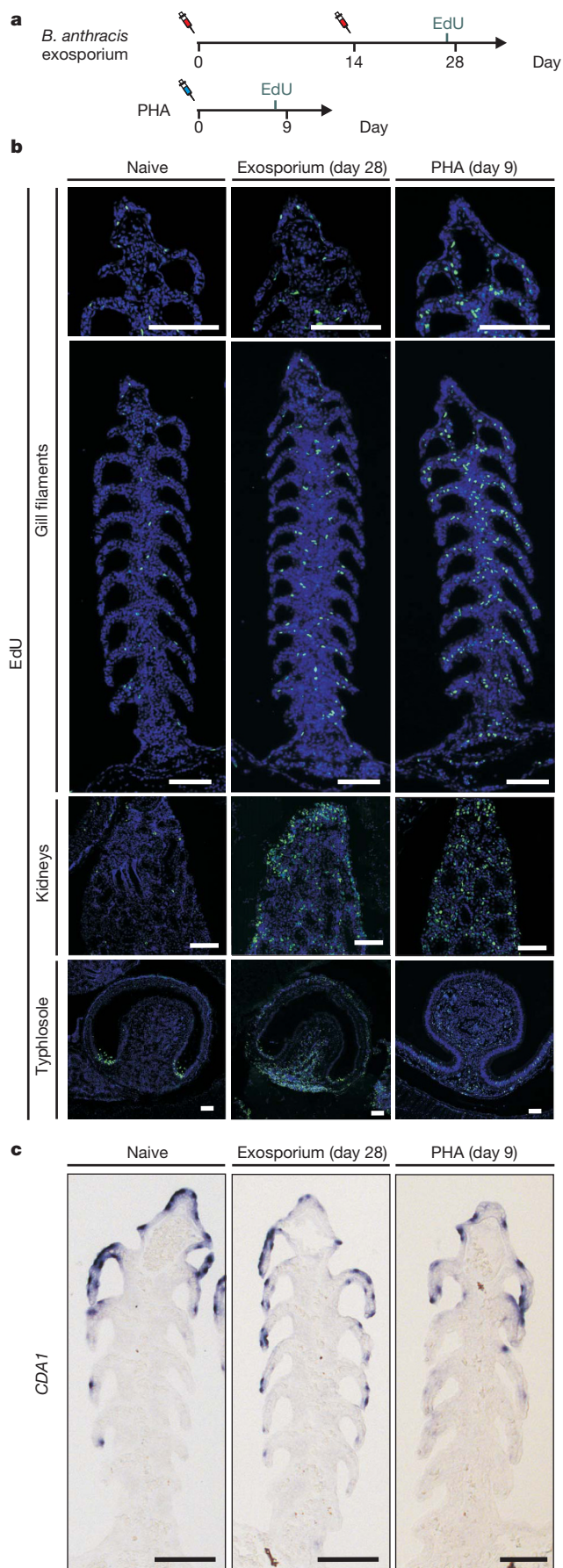


Figure 4 | Selection of VLRA-expressing lymphocytes in the thymoid.

a, Micrographs showing the site of tissue procurement, by laser-capture microdissection (LCM), at the gill filament tip region of the thymoid. Scale bars, 50 μ m. **b**, Proportion of non-productive sequences among assembled VLRA genes. The difference between the thymoid and blood is significant at $P < 0.01$ (Fisher's exact test) (thymoid, $n = 29$; blood, $n = 18$; n , number of sequences). ND, not detectable. **c**, Apoptotic cells (left), as detected with anti-caspase-3 antibody (red), preferentially occur in the thymoid, as detected by CDA1 expression (centre, blue). In the left panel, DNA is counterstained with DAPI (blue). In the centre panel, anatomical landmarks are indicated: tip of gill filament (t), first secondary lamella (1), second secondary lamella (2) and so on. A numerical analysis of the distributions of caspase-3-positive and CDA1-expressing cells relative to the relevant anatomical landmarks of gill filaments is shown in the right panel; randomly selected sections were used (caspase-3, $n = 36$; CDA1, $n = 17$; n , number of sections; error bars, s.e.m.). Scale bars, 100 μ m. **d**, Assembled VLRA genes are detectable in VLRA⁻VLRB⁻ (double negative, DN) cells separated by FACS after isolation from the blood or gills of lamprey larvae but not in VLRA⁻VLRB⁺ (B⁺) cells. **e**, Non-productive assemblies of VLRA genes predominate in VLRA⁻VLRB⁻ cells. By contrast, in VLRA⁺VLRB⁻ cells, essentially all assembled VLRA genes are productive. VLRA⁻VLRB⁻ cells, $n = 42$ for gills, $n = 33$ for blood; VLRA⁺VLRB⁻ cells, $n = 33$ for gills, $n = 39$ for blood; n , number of sequences. Samples are from *L. planeri* in **a** and **b** and *P. marinus* in **c-e**.

Figure 3 | Stimulation does not affect cell proliferation and gene expression in the thymoid of *P. marinus*. **a**, Time points for injection with *B. anthracis* exosporium, the lectin PHA and the nucleoside analogue 5-ethynyl-2'-deoxyuridine (EdU). **b**, Representative sections revealing the number and location of proliferating cells (EdU, green), as determined by immunofluorescence microscopy. DNA is stained with Hoechst stain (blue). The tips of the gill filaments are shown at higher magnification in the upper panels. **c**, Distribution of CDA1-expressing cells in gill filaments, as determined by RNA *in situ* hybridization with a gene-specific riboprobe. Scale bars, 100 μ m.

and why it was revealed only by extensive gene expression analyses. The identification of the thymoid in lampreys provides a starting point for more detailed comparative studies between jawless and jawed vertebrates, guided by the wealth of information about thymopoiesis in jawed vertebrates. Finally, these findings suggest that a common vertebrate ancestor had not only T-like and B-like lymphocyte lineages but also anatomically distinct tissues in which these cells could develop in a spatially segregated manner.

METHODS SUMMARY

Lampetra planeri larvae were sampled in the Freiburg area (Germany). *Petromyzon marinus* larvae were collected from tributaries to Lake Michigan (Michigan). RNA *in situ* hybridization analyses were performed on paraffin-embedded tissue sections. Specific antibodies were used to detect VLRA⁺ and VLRB⁺ lymphocytes *in situ*. Cells undergoing apoptosis were detected with caspase-3-specific antibodies, and proliferating cells were marked by incorporation of 5-ethynyl-2'-deoxyuridine and detected by Click-iT reaction. Preparative flow cytometry was used to separate lymphocyte populations according to their VLRA and VLRB expression. PCR with specific primers was used to amplify germ-line and assembled forms of VLRA genes for subsequent cloning and sequence analysis. Laser-capture microdissection of paraffin-embedded tissue sections was used to procure genomic DNA from specific regions. Transmission electron microscopy was used for high-resolution tissue analysis.

Full Methods and any associated references are available in the online version of the paper at www.nature.com/nature.

Received 2 May; accepted 8 November 2010.

1. Finstad, J. & Good, R. A. The evolution of the immune response. III. Immunologic responses in the lamprey. *J. Exp. Med.* **120**, 1151–1168 (1964).
2. Mayer, W. E. *et al.* Isolation and characterization of lymphocyte-like cells from a lamprey. *Proc. Natl Acad. Sci. USA* **99**, 14350–14355 (2002).
3. Pancer, Z. *et al.* Somatic diversification of variable lymphocyte receptors in the agnathan sea lamprey. *Nature* **430**, 174–180 (2004).
4. Pancer, Z. *et al.* Variable lymphocyte receptors in hagfish. *Proc. Natl Acad. Sci. USA* **102**, 9224–9229 (2005).
5. Guo, P. *et al.* Dual nature of the adaptive immune system in lampreys. *Nature* **459**, 796–801 (2009).
6. Alder, M. N. *et al.* Diversity and function of adaptive immune receptors in a jawless vertebrate. *Science* **310**, 1970–1973 (2005).
7. Cooper, M. D. & Alder, M. N. The evolution of adaptive immune systems. *Cell* **124**, 815–822 (2006).
8. Nagawa, F. *et al.* Antigen-receptor genes of the agnathan lamprey are assembled by a process involving copy choice. *Nature Immunol.* **8**, 206–213 (2007).
9. Rogozin, I. B. *et al.* Evolution and diversification of lamprey antigen receptors: evidence for involvement of an AID-APOBEC family cytosine deaminase. *Nature Immunol.* **8**, 647–656 (2007).
10. Bajoghli, B. *et al.* Evolution of genetic networks underlying the emergence of thymopoiesis in vertebrates. *Cell* **138**, 186–197 (2009).
11. Boehm, T. & Bleul, C. C. The evolutionary history of lymphoid organs. *Nature Immunol.* **8**, 131–135 (2007).
12. Nehls, M. *et al.* Two genetically separable steps in the differentiation of thymic epithelium. *Science* **272**, 886–889 (1996).
13. Schaffer, J. Über die Thymusanlage bei *Petromyzon planeri*. Zweite vorläufige Mittheilung über den feineren Bau des Thymus. *Sber. K. Akad. Wiss.* **103**, 149–156 (1894).
14. Wallin, I. E. The relationships and histogenesis of thymus-like structures in ammocoetes. *Am. J. Anat.* **22**, 127–167 (1917).
15. Alder, M. N. *et al.* Antibody responses of variable lymphocyte receptors in the lamprey. *Nature Immunol.* **9**, 319–327 (2008).
16. Kishishita, N. *et al.* Regulation of antigen-receptor gene assembly in hagfish. *EMBO Rep.* **11**, 126–132 (2010).
17. Kasamatsu, J. *et al.* Identification of a third variable lymphocyte receptor in the lamprey. *Proc. Natl Acad. Sci. USA* **107**, 14304–14308 (2010).

Supplementary Information is linked to the online version of the paper at www.nature.com/nature.

Acknowledgements We thank C. Happe and M. Held for technical help, C. L. Turnbough Jr for providing *B. anthracis* spores and exospores, and the Emory University School of Medicine core facility for flow cytometry for cell-sorting services. This work was supported by the Max Planck Society, the Deutsche Forschungsgemeinschaft, the National Institutes of Health and the Georgia Research Alliance.

Author Contributions B.B., P.G., N.A., M.H., C.S., N.M., D.E.B., M.S., M.D.C. and T.B. designed the experiments, performed the research, analysed the data and wrote the manuscript.

Author Information Reprints and permissions information is available at www.nature.com/reprints. The authors declare no competing financial interests. Readers are welcome to comment on the online version of this article at www.nature.com/nature. Correspondence and requests for materials should be addressed to T.B. (boehm@immunbio.mpg.de).

METHODS

Animals and immune stimulation. *Lampetra planeri* (5–12 cm long and 1–3 years of age) were sampled in the Freiburg area (Germany) with the permission of the local authorities. *Petromyzon marinus* larvae (8–12 cm long and 2–4 years of age) were from Lake Michigan tributaries in Michigan (Lamprey Services). Fish were maintained in sand-lined aquaria at 18 °C and fed brewer's yeast. Larvae were immunized with *Bacillus anthracis* exosporium or stimulated with phytohaemagglutinin (PHA) (Sigma) as described previously⁴. Briefly, larvae were anaesthetized with 0.1 g l⁻¹ ethyl 3-aminobenzoate methanesulphonate (MS-222) (Sigma) and were given 60 µl intracoelomic injections of *B. anthracis* exosporia (10 µg) or PHA-L (leukoagglutinin; 25 µg) prepared in sterile 0.67× PBS buffer. Immunization with exosporia was carried out on day 0 and 14, and tissues were collected after animals were killed by administering 1 g l⁻¹ MS-222 on day 28. PHA was administered as a single injection, and animals were killed on day 9 after injection. For proliferation assays, lampreys were injected with 5-ethynyl-2'-deoxyuridine (EdU) (5 µg) (Invitrogen) in 60 µl 0.67× PBS and returned to aquaculture for 24 h before being killed.

Flow cytometry and cell sorting. Leukocytes were isolated from the blood and other tissues of *P. marinus* larvae before being separated by FACS as previously described⁵. Briefly, blood was collected in 0.67× PBS containing 30 mM EDTA, and buffy coats were prepared by centrifugation at 50g. Leukocytes were liberated from gills by mincing with frosted glass slides. Cells were stained with R110 anti-VLRA rabbit polyclonal serum and 4C4 anti-VLRB mouse monoclonal antibody, followed by R-phycoerythrin-conjugated goat anti-rabbit antibody and allophycocyanin-conjugated goat anti-mouse antibody (SouthernBiotech), and then were sorted into VLRA⁺, VLRB⁺ and VLRA⁻VLRB⁻ populations on a FACSAria II flow cytometer (Becton Dickinson).

Genomic DNA and PCR. Genomic DNA was extracted from sorted cell populations—VLRA⁺, VLRB⁺ and VLRA⁻VLRB⁻ cells in the lymphocyte gate of blood and gill samples from *P. marinus*—using a DNeasy kit (QIAGEN). First-round PCR was carried out with VLRA-F and VLRA-R primers (and Ex Taq polymerase, Takara). Reactions were amplified using the following: one cycle of 94 °C for 1 min; 35 cycles of 94 °C for 15 s, 56 °C for 20 s and 72 °C for 1 min; and one cycle of 3 min at 72 °C. Second-round (nested) PCR was performed with VLRA-F2 and VLRA-R2 primers. Reactions were amplified using the following: one cycle of 94 °C for 1 min; 35 cycles of 94 °C for 15 s, 57 °C for 20 s and 72 °C for 1 min; and one cycle of 3 min at 72 °C. PCR products were cloned into the pGEM-T vector (Promega). Paraffin-embedded sections (5–7 µm) of *L. planeri* were used for laser-capture microdissection as previously described¹⁸. Genomic DNA extraction was performed using a PicoPure DNA extraction kit (Arcturus). VLRA genes from *L. planeri* tissues were amplified by nested PCR, the first amplification using primers vlra_1f and vlra_2r, the second amplification using primers vlra_3f and vlra_4r. Reactions were amplified using the following: first amplification, one cycle of 96 °C for 2 min; 35 cycles of 96 °C for 15 s, 60 °C for 30 s and 72 °C for 2 min; and one cycle of 5 min at 72 °C; and second amplification, as above but for 25 cycles instead of 35. The assembled VLRA gene fragments were then cloned into the pGEM-T vector. Clones were sequenced using the ABI 3730xl DNA Analyzer (Applied Biosystems). Primer sequences are listed in Supplementary Table 1.

Immunofluorescence microscopy. For analysis of lymphocyte distribution in *P. marinus* larvae, dissected tissues were fixed for 12 h in 0.67× PBS containing 2% paraformaldehyde at 4 °C, cryopreserved in 30% sucrose, embedded in OCT compound (Tissue-Tek, Sakura) and sectioned at 7 µm on a cryostat (Thermo). Sections were permeabilized in PBS containing 10% goat serum, 0.5% saponin, 10 mM HEPES buffer and 10 mM glycine. They were stained for 1 h with R110 and 4C4 antibodies, followed by 1 h with the appropriate Alexa-Fluor-conjugated secondary antibodies (Invitrogen) before being mounted in ProLong Gold with 4',6-diamidino-2-phenylindole (DAPI) solution (Invitrogen). Fluorescence microscopy was performed with an Axiovert 200M microscope (Zeiss), equipped with a ×40 objective (numerical aperture, 0.6; ocular magnification, ×10).

For detection of apoptotic cells, frozen sections (10–15 µm) were fixed in 4% paraformaldehyde for 15 min, washed several times in PBS, and permeabilized with PBS containing 0.2% Triton X-100 detergent for 5 min, then washed again in PBS. To block non-specific binding sites, the sections were incubated for 1 h in 5% normal goat serum diluted in blocking solution (PBS containing 0.1% Tween 20 detergent). Sections were then incubated with rabbit anti-active caspase-3 (G7481, Promega; at a 1:250 dilution in blocking solution) for 16 h at 4 °C. After washing in PBS containing 0.1% Tween 20, a Cy3-conjugated donkey anti-rabbit antibody (1:500 in blocking solution) was applied for 30 min. Sections were washed several times in PBS and, after drying, were mounted in Fluoromount-G and 4',6-diamidino-2-phenylindole (DAPI). Micrographs were taken using an Axio Imager.Z1 and ApoTome microscope (Zeiss).

For analysis of cell proliferation, lampreys were embedded in OCT and cryosectioned. EdU detection was performed using the Click-iT EdU Alexa Fluor 488 Flow Cytometry Assay Kit (Invitrogen). Briefly, frozen sections (10–15 µm) were fixed with 4% paraformaldehyde for 15 min at 20 °C and washed in PBS. Sections were permeabilized with PBS containing 0.5% Triton X-100 and then washed in PBS. Sections were then incubated with the EdU reaction cocktail for 30 min at 20 °C. After several washes in PBS, sections were incubated in Hoechst stain (1:2,000 in PBS) for 30 min. Sections were washed several times in PBS and, after drying, were mounted with Fluoromount-G. For EdU detection in paraffin-embedded tissue, sections were deparaffinized and rehydrated, and then permeabilized and processed as above. Images were processed with the program Photoshop (Adobe).

Electron microscopy. Killed *P. marinus* larvae were immersed in Karnovsky's fixative (paraformaldehyde and glutaraldehyde) for 2 h. Thin cross sections were cut from gill regions and prepared for transmission electron microscopic analysis as described previously¹⁹. Sections were examined with a JEM-1230 transmission electron microscope (JEOL). Images were recorded digitally using the UltraScan 4000 imaging system (Gatan).

In situ hybridization analysis. RNA *in situ* hybridization was performed with digoxigenin (DIG)-labelled RNA riboprobes as described previously¹⁰. Probe sequences are listed in Supplementary Table 2. For *DLL-B* and *CDAI1* colocalization studies, *in situ* hybridization was carried out by use of short gene-specific locked-nucleic-acid (LNA)-enhanced oligonucleotides (Exiqon; see Supplementary Table 2) as described previously¹⁰, with the exception that the temperature of hybridization was 54 °C. Double *in situ* hybridization was carried out as follows. DIG- and fluorescein isothiocyanate (FITC)-labelled RNA antisense probes were hybridized to RNA in tissue sections simultaneously. The DIG-labelled probe was detected first, with an alkaline-phosphatase-conjugated anti-DIG antibody (1:2,000 dilution in maleic acid buffer (MAB); 100 mM maleic acid, pH 7.5, 150 mM NaCl, 2 mM Levamisol, 0.1% Tween 20 and 1% blocking reagent (Roche)). It was revealed by staining with BM Purple (Roche), according to the manufacturer's instructions. The sections were washed several times with TNT solution (10 mM Tris-Cl, pH 7.5, 500 mM NaCl and 0.1% Tween 20), and the FITC-labelled probe was detected by a peroxidase-conjugated anti-FITC antibody (1:500 dilution in MAB) and revealed by Cy5 fluorescence, using Tyramide Signal Amplification Plus Cy5 system (Perkin Elmer). For three-dimensional reconstructions, alternate (5 µm) sections were hybridized with gene-specific LNA-enhanced oligonucleotides. After the staining reactions, the thymoid regions of the gill filaments were photographed using an Imager Z1 microscope (Zeiss). A series of TIF files indicating the positions of the *CDAI1*- and *DLL-B*-expressing cells, and the boundaries of neighbouring cells, were generated using the program CoreDRAW Graphics Suite 11. Each series of images was aligned using DeltaViewer software (<http://delta.math.sci.osaka-u.ac.jp/DeltaViewer/>) to build the three-dimensional image.

18. Espina, V. *et al.* Laser-capture microdissection. *Nature Protocols* **1**, 586–603 (2006).
19. Bockman, D. E. & Cooper, M. D. Pinocytosis by epithelium associated with lymphoid follicles in the bursa of Fabricius, appendix, and Peyer's patches. An electron microscopic study. *Am. J. Anat.* **136**, 455–477 (1973).